JOURNAL OF Materials CHEMISTRY

Molecular recognition of adenine, adenosine and ATP at the air–water interface by a uracil appended fullerene

Renata Marczak,[b] Vu T. Hoang,[a] Krzysztof Noworyta,[b] Melvin E. Zandler,[a] Wlodzimierz Kutner*[b] and Francis D'Souza*[a]

[a]*Department of Chemistry, Wichita State University, 1845 Fairmount, Wichita, KS, 67260-0051, USA. E-mail: Francis.DSouza@Wichita.edu; Fax: +1 (316) 978-3431; Tel: +1 (316) 978-7380*

[b]*Institute of Physical of Chemistry, Polish Academy of Sciences, Kasprzaka 44/52, 01-224 Warsaw, Poland. E-mail: wkutner@ichf.edu.pl*

Received 8th March 2002, Accepted 22nd April 2002
First published as an Advance Article on the web 10th May 2002

A new C_{60}-uracil adduct capable of hydrogen bonding, *via* complimentary base pairing, of adenine, adenosine, and adenosine 5′-triphosphate (ATP) was synthesized and characterized by UV-visible and ^{1}H NMR spectroscopy, cyclic voltammetry and differential pulse voltammetry, as well as ESI-mass spectrometry. Molecular modeling by *ab initio* B3LYP/3–21G(*) calculations revealed the Watson–Crick type base pairing. Stable "expanded liquid" Langmuir films of the C_{60}-uracil–adenine, C_{60}-uracil–adenosine and C_{60}-uracil–ATP complexes were prepared and characterized by isotherms of surface pressure *versus* area per molecule as well as the Brewster angle microscopy imaging. The area per molecule at infinite adduct dilution in the film was dependent on composition of the subphase solution and increased in the order: water < adenine < adenosine < ATP solution. Comparison of experimental and calculated areas per molecule and dipole moment components normal to the subphase–air interface indicated prevailing horizontal orientation of the complexes in the films. The Langmuir films were transferred, by using the Langmuir–Blodgett technique, onto quartz slides and characterized by the UV-visible spectroscopy.

1 Introduction

Hydrogen bonding *via* complementary base pairing plays decisive roles in biological molecular recognition, such as replication of nucleic acids, maintenance of tertiary structure of proteins, and enzymatic substrate recognition.[1] The hydrogen bonding involved in the base-pairing is a highly directional secondary valence force compared with other non-covalent bonding, such as electrostatic, van der Waals, and hydrophobic interactions. This directionality in intermolecular interactions is crucial for specific molecular recognition.[1] In fact, hydrogen bonding has been used effectively in artificial recognition systems.[2] In this regard, molecular probes attached to nucleic acid bases have been employed for studying protein interactions, and also, in studies related to DNA cleavage, model electron transfer reactions, *etc.*[3] Often, photosensitizing molecules attached to nucleic acid bases have been utilized in such studies.[3a]

During the last decade, several groups have reported on novel physico-chemical properties of fullerenes.[4] Fullerenes offer several unique properties, such as a large size, hydrophobicity, three-dimensionality, electronic effects, and rich redox- and photochemistry. Hence, utilization of fullerenes as probes in biological studies has attracted increasing attention, especially in the fields of DNA cleavage, photodynamic therapy, HIV treatment, neuroprotections and apoptosis.[5] These applications are especially possible given the strong ground state light absorption of fullerene.[6] Also, upon excitation, fullerenes form long-living triplet states of lifetimes ranging between 50 and 100 μs that are considered to be cytotoxic agents in photodynamic therapy.[6] However, in order to make use of fullerenes for potential biological or medicinal applications, they need to be functionalized to bear a receptor unit, offering high binding affinity and selectivity.

Several elegant fullerene derivatives bearing receptor units have already been synthesized and their interactions with DNA have been reported.[5–7] Moderate DNA photocleavage activity in some cases has been observed. Studies so far performed have indicated that the distance between the fullerene probe and the binding units (oligonucleotide chain, polyethylene glycol derivatives, groove binders, acridine, *etc.*) may be critical for modulating DNA interactions.

In the present study we have derivatised fullerene to bear a uracil (thymine) receptor unit. This unit is targeted to base-pair with an adenine residue of DNA or a nucleotide through the Watson–Crick type pairing, thus offering much needed selectivity (Scheme 1). However, it is essential to understand the base-paring mechanism prior to studies involving DNA or protein interactions. Therefore, we have performed here both computational and experimental studies of base-pairing

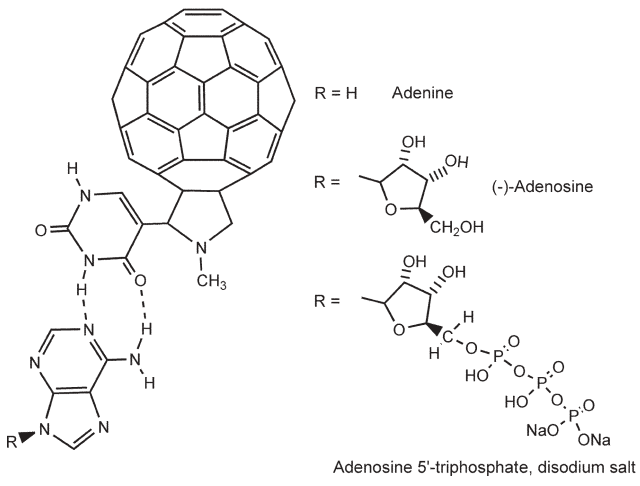

Scheme 1

involving the newly synthesized fullerene-uracil adduct and adenine, adenosine or ATP. The interfacial molecular recognition[8] studied here in the Langmuir films is of significance since it takes advantage of unique physico-chemical characteristics of interfaces and, moreover, it furthers our understanding of biological recognition which in many cases takes place at the surface of biological macromolecules.

The present Langmuir film studies of the fullerene adduct are also useful for exploring the possibility of fullerene applications in materials science because the Langmuir technique permits one to prepare films with well-defined structure and molecularly controlled thickness. The Langmuir–Blodgett (LB) technique allows one to fabricate mono- or multilayer films onto various solid substrates for optical, electrochemical and photochemical investigations. In this regard, studies on several fullerene derivatives have been performed aiming at their structural characterization, interfacial electron transfer, ion transport, *etc.*[9] Ordered films of such derivatives could find applications as active surface layers in microsensors or optoelectronic devices, as materials for generating second-order nonlinear optical response and as surface coatings to provide or protect bulk material from the environment.

2 Experimental

Chemicals

Fullerene, C_{60}, used in the synthesis was from BuckyUSA (Bellaire TX, USA). Adenine, (−)-adenosine, the disodium salt of adenosine 5′-triphosphate (ATP), 5-formyl uracil, sarcosine, and 1,2-dichlorobenzene in a "sure seal" bottle were from Aldrich Chemical Co. (Milwaukee WI, USA). Supporting electrolyte salts, *i.e.*, tetra(*n*-butyl)ammonium hexafluorophosphate, (TBA)PF_6, (98% purity) from Fluka (Buchs, Switzerland) and KPF_6 from Aldrich were dried under reduced pressure at 40 °C and stored in a vacuum desiccator. A HPLC grade acetonitrile (+99% purity, water content < 0.005%) from Merck (Darmstadt, Germany) was stored over molecular sieves 4 Å. Analytical grade chloroform from POCH (Gliwice, Poland) was used as received. Water used for preparation of solutions of a Langmuir film subphase was distilled and further purified (18.2 MΩ cm) with a Milli-Q filtering system of Millipore Corp. (Bedford MA, USA), which was equipped with one carbon and two ion-exchange cartridge stages. Argon "analyzed" for deaeration of solutions for electrochemical investigations was from Multax, s.c. (Stare Babice, Poland).

Synthesis of 2-(5′-uracil)fulleropyrrolidine, 1

Adduct **1** (C_{60}-uracil) was prepared according to a general procedure of fulleropyrrolidine synthesis developed by Prato and coworkers.[10] That is, a mixture of C_{60} (100 mg), sarcosine (31 mg), and 5-formyl uracil (35 mg) in toluene (60 ml) was refluxed for about 12 h. Then, the solvent was removed under reduced pressure. The crude product was dissolved in toluene and purified, with 20% yield, over a silica gel column using a mixture of ethyl acetate and toluene as eluent. Further purification of **1**, needed for the Langmuir film studies, was carried out on a semi-preparative HPLC, 10 × 250 mm, Cosmosil Buckyprep column of Nacalai Tesque (Kyoto, Japan) with an acetonitrile–toluene (1 : 3, *v* : *v*) eluent at a 4.5 mL min^{-1} flow rate and 1 mL volume of samples injected with a Model 7125 syringe loading injector of Rheodyne (Cotati CA, USA). The isocratic HPLC system used was composed of a 6000A pump of Waters (Millipore Corp., Milford MA, USA) and a SPD10A UV-visible detector of Shimadzu Corp. (Tokyo, Japan) set at 340 nm. ^{1}H NMR in CS_2 : $CDCl_3$ (1 : 1, *v* : *v*), δ ppm: 8.63 (s, 1H), 4.91 (s, 1H), 4.95, 4.25 (d, d, 2H), 2.77 (s, 3H). ESI-MS in CH_2Cl_2, calcd. 887, found 887 (8%), 854.2 (100%, M − 2O), 777.1 (14%, M − uracil). UV-vis in CH_2Cl_2, λ_{max}, nm, 325(sh), 415, 445 nm.

Apparatus and procedures

The Langmuir films of **1** floating on the subphase of pure water or the water solution of 1.81 mmol dm^{-3} adenine, adenosine or ATP were prepared by using a computerized system of 601BAM trough (total area 490 cm^2) of Nima Technology, Ltd. (Coventry, UK). Surface pressure was measured with an accuracy of ±0.1 mN m^{-1} by using a PS4 sensor (Nima) of a Wilhelmi plate type. Surface potential was measured with an accuracy of ±10 mV by using a KP-2 sensor (Nima) of a Kelvin probe type. The surface of the subphase solution was cleaned by repeated compressing, aspirating of traces of surface active impurities and expanding prior to spreading 0.1 to 0.5 mL of a sample of 0.114 mmol dm^{-3} C_{60}-uracil in chloroform. Changes of surface pressure of the blank subphase solutions used were lower than 0.2 mN m^{-1} in the cleaning compression–expansion cycles. Then, chloroform was allowed to evaporate for 15 min and isotherms of surface pressure (π) against area per molecule (A) were recorded, under a compression–expansion regime, at a rate of 25 cm^2 min^{-1}.

Morphology changes of surfaces of the Langmuir films during compression and expansion were imaged with the Brewster angle microscopy by using a MiniBAM microscope of NFT-Nanofilm Technologie GmbH (Göttingen, Germany) of the 20 μm resolution. The Langmuir films of **1** were transferred with a D1L linear dipper of Nima by using the Langmuir–Blodgett (LB) technique, at the surface pressure of 15 mN m^{-1} and transfer rate of 5 mm min^{-1}, onto 12 × 10 × 1 mm quartz slides for the UV-vis spectroscopy measurements with a UV-3100 spectrophotometer of Shimadzu Corp. (Tokyo, Japan).

For cyclic voltammetry (CV) and differential pulse voltammetry (DPV) measurements of **1** in solution, a conventional three-electrode electrochemical mini cell was used with a 1 mm diameter glass sealed Au disk electrode, Pt wire and Ag wire which served as the working, auxiliary and pseudo reference electrode, respectively. Solutions were deaerated with an argon purge prior to all electrochemical measurements. The potentials are reported with respect to the formal redox potential of the ferrocene/ferrocenium (Fc/Fc^+) couple that was used as an internal standard for potentials. All experiments were performed at 20 ± 1 °C by air conditioning of the laboratory room.

The computational modeling of base-pairing was performed by *ab initio* B3LYP/3–21G(*) methods with the GAUSSIAN 98[11] software package on an SGI ORIGIN 2000 computer and various PC's. The area per molecule of both **1** and its complexes containing bases for Langmuir studies was calculated by using HyperChem Release 5 of Hypercube, Inc. (Gainesville FL, USA) by PM3 methods.

3 Results and discussion

The structural integrity of the newly synthesized C_{60} derivative, 2-(5′-uracil)fulleropyrrolidine, **1**, was derived from ^{1}H NMR spectroscopy, ESI-mass spectrometry, optical absorption and electrochemical results. The ^{1}H NMR spectral data revealed peaks corresponding to the pyrrolidine ring and the uracil receptor units. The ESI-MS spectrum of **1** in the CH_2Cl_2 matrix revealed peaks corresponding to the molecular ion and its fragments. The optical absorption spectrum of **1** in CH_2Cl_2 revealed peaks at 325 (sh), 415 and 445 nm, typical of fulleropyrrolidine derivatives. No peak corresponding to the uracil moiety at 325 nm was observed. Presumably, such peaks were masked by the intense absorption bands of fulleropyrrolidine in the 300–450 nm region.

The CV and DPV behavior of **1** in 0.1 mol dm^{-3} (TBA)PF_6, in a mixed solvent solution of toluene and acetonitrile (4 : 1,

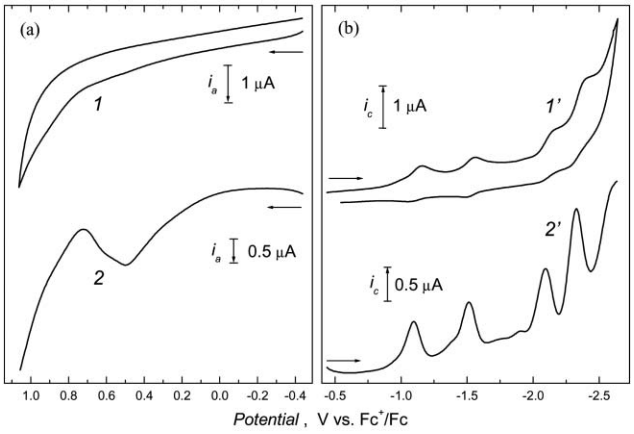

Fig. 1 Cyclic voltammetry curves *1* and *1′* at 0.02 V s^{-1} potential scan rate and differential pulse voltammetry curves *2* and *2′* at 50 mV pulse amplitude and 50 ms pulse duration for 0.5 mmol dm^{-3} C_{60}-uracil in 0.1 mol dm^{-3} (TBA)PF_6, in toluene–acetonitrile (4 : 1, *v* : *v*) in the (a) anodic and (b) cathodic potential range.

v : *v*), was examined both in the positive and negative potential range for investigation of electrochemical properties of both the uracil and fullerene part of the adduct, respectively.

In the positive potential range, there is an irreversible anodic, poorly developed, CV (curve *1* in Fig. 1a) and much better developed DPV (curve *2* in Fig. 1a) current signal composed of at least two merged peaks at *ca.* 0.49 and 0.60 V *vs.* Fc/Fc^+ of electro-oxidation. This signal may correspond to electro-oxidation of both the pyrrolidine and uracil part of the adduct, respectively, since it is close to that found for *N*-methyl-2-butylfulleropyrrolidine at 0.45 V (ill-defined) and that for free uracil at *ca.* 0.50 V and 0.60 V under the same solution conditions (not shown). Apparently, the fullerene moiety in **1** has no appreciable effect on the redox properties of the uracil-pyrrolidine entity.

During the negative potential excursion, four one-electron CV (curve *1′* in Fig. 1b) and DPV (curve *2′* in Fig. 1b) redox couples are clearly developed in the accessible potential window, similar to that of the parent C_{60}. Formal redox potentials of these couples are located at −1.20, −1.60, −2.18, and −2.45 V *vs.* Fc/Fc^+ and correspond to the 0/−, −/2−, 2−/3− and 3−/4− redox states, respectively, by analogy to the redox couples of genuine C_{60} which are at −1.04, −1.46, −1.77, and −1.97 V *vs.* Fc/Fc^+ under the same solution conditions (not shown). Importantly, formal redox potentials of the first two couples are shifted only by −0.16 and −0.14 V while those of the last two couples by as much as −0.42 and −0.48 V with respect to formal redox potentials of the corresponding C_{60} couples. The presently found shifts are in agreement with those reported earlier for other fulleropyrrolidine derivatives.[12]

Ab initio B3LYP/3–21G(*) modeling of the C_{60}-uracil–adenine base paired complexes

The molecular recognition directed base pairing of **1** and adenine, applied as one of the complex bases, has been modeled by using density functional methods at the B3LYP/3–21G(*) level. The density function theory (DFT) methods were chosen over the Hartree–Fock or semi-empirical approaches since recent studies have shown that the DFT-B3LYP method at the 3–21G(*) level more accurately predicts the molecular geometry and electronic structure of fullerene and porphyrin derivatives.[13] For the modeling purpose, the starting adduct **1** and adenine were, first, fully optimized to a stationary point on the Born–Oppenheimer potential energy surface and, then, allowed to interact. Fig. 2 shows the energy optimized structure of **1** interacting with adenine to form a complex which reveals the Watson–Crick type base pairing.

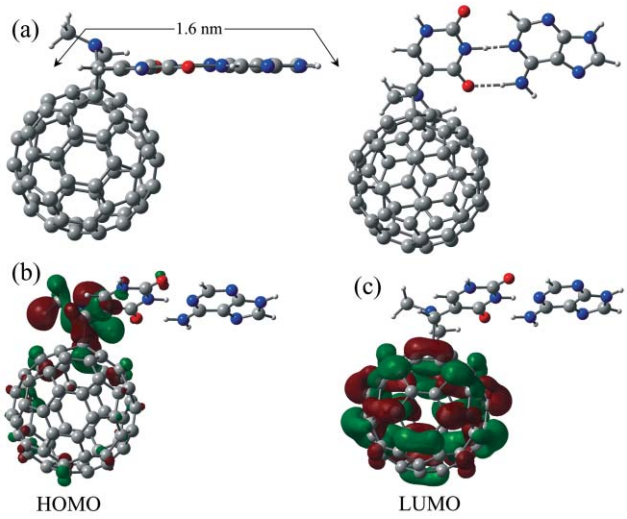

Fig. 2 *Ab initio* B3LYP/3-21G(*) energy optimized (a) structure, (b) HOMO and (c) LUMO of the C_{60}-uracil–adenine complex.

In the base-paired C_{60}-uracil–adenine complex, the uracil and adenine rings are positioned in a plane and do not reveal any steric constraints due to the presence of the bulky fullerene spheroidal entity (Fig. 2a). The H-bond distances for the base pairs, *i.e.*, N–H···O and N–H···N, are calculated as 1.85 and 1.58 Å, respectively, suggesting formation of a stable Watson–Crick type base paired complex. Interestingly, a non-Watson–Crick structure corresponding to 180° rotation of the adenine group around the N–H···N bond has virtually the same hydrogen bond distances, dissociation energy, and MO structure as the Watson–Crick assembly compared to the non-Watson–Crick pairing. The Watson–Crick structure of the uracil–adenine pair and the 5-(2-pyrrolidine)uracil–adenine pair are calculated to be lower by 0.6 kcal mol^{-1} but higher by 0.6 kcal mol^{-1} for the C_{60}-uracil–adenine complex.

For **1**, the low energy conformer, out of the four possible conformers, is the one in which the pyrrolidine ring is puckered in such a way that the 2-uracil (thymine) group is *syn* to the nitrogen atom and the N–CH_3 group is *trans* to the 2-uracil group. Earlier, such a conformation for a fulleropyrrolidine derivative was confirmed by X-ray structural analysis.[14] Rotation of the uracil group of **1** by 180° around the connecting C–C bond to the pyrrolidine ring resulted in a higher energy conformation.

The complex formation energy for the base pair formation, *i.e.*, the difference between the energy of the C_{60}-uracil–adenine complex and the sum of the energies of **1** and adenine was calculated to be −29.1 kcal mol^{-1} suggesting formation of a stable complex of similar geometry and bond strength as the adenine–uracil hydrogen bonded complex. The corresponding B3LYP/3-21G(*) complexation energies for the formamide dimer, the cytosine dimer, the uracil–adenine complex, and the pyrrolidine-uracil–adenine complex are −28.9, −31.4, −28.6 and −28.4 kcal mol^{-1}, respectively, compared to the high level BSSE corrected results at the MP2/6-311++G (3df, pd) level of Sponer and Hobza[15] of −13.0, −18.8 and −13.9 kcal mol^{-1} for the first three complexes. The B3LYP/3–21G(*) complexation energies reported here are known to be systematically high for several reasons, mainly due to effects of the small basis set, the negligence of Basis Set Superposition Error (BSSE), and the reported inability of B3LYP to "properly capture the intersystem electron correlation effects". The magnitude of these effects was explored by comparing computations of the formamide and cytosine dimers, and the uracil–adenine complex at various levels with different bases sets with the high level results of Sponer and Hobza.[15] The correlation effects are, fortuitously, nearly correct at the B3LYP/3–21G(*) level; that is, for the formamide and cytosine dimers and the

uracil–adenine complex the B3LYP-HF difference is about +6.0 kcal mol^{-1} at the 3-21G(*) basis and +4.0 kcal mol^{-1} at the 6–31G* and 6–31G** bases compared to the MP2-HF difference of +2.5 kcal mol^{-1} at the 6–31G** basis and +5.4 kcal mol^{-1} at the 6–311**G (3df, pd) level. However, the 3–21G(*) basis overestimates the deformation (relaxation) energy by about 1 kcal mol^{-1} and is subject to a high BSSE of about +11.0 kcal mol^{-1} compared to +6.3 kcal mol^{-1} at the 6–31G* (.25),[15] +2.6 kcal mol^{-1} at the 6.31G**, +2.1 at the MP2/6–31+G(2d, p)[16] and +1.9 kcal mol^{-1} at the cc-pVTZ bases. The B3LYP/3–21G(*) results, therefore, agree with higher level calculations that the complexation energy of the C_{60}-uracil–adenine is slightly higher than that of uracil–adenine with a probable magnitude of *ca.* −14.0 kcal mol^{-1} compared to −13.1 kcal mol^{-1} for uracil–adenine.[16] Importantly, the theoretically estimated complexation energy of the C_{60}-uracil–adenine complex and that of the reference uracil–adenine complex are comparable, suggesting that the stability constant of the C_{60}-uracil–adenine complex is not significantly different from the uracil–adenine complex ($K \sim 10^2$ in aqueous solution). Our attempts to determine the K value by ^{1}H NMR spectroscopy were unsuccessful due to the insolubility of adenine, adenosine or ATP in deuterated organic solvents such as $CDCl_3$.

The calculated HOMO and LUMO for the C_{60}-uracil–adenine complex are shown in Fig. 2b and c. As in **1**, the majority of the HOMO is located on the pyrrolidine ring with a small portion on the C_{60} and uracil ring atoms. However, the LUMO is entirely located on the C_{60} spheroid. The HOMO energy of **1**, being equal to −5.93 eV, reveals a slight change, that is, it is −5.80 eV after base pairing of the adduct with adenine. The edge-to-edge distance, that is the overall size (see Fig. 2a) of the C_{60}-uracil–adenine complex, was estimated to be around 1.6 nm. This value is close to that obtained from the Hyperchem PM3 calculations, used to estimate area per molecule in the Langmuir film studies described below.

Langmuir films of C_{60}-uracil base paired complexes

A series of π–A isotherms were recorded for the adduct films prepared by spreading a 0.2 mL sample of 0.114 mmol dm^{-3} **1** in chloroform onto pure water or the adenine, adenosine or ATP aqueous solutions of the same concentration of 1.81 mmol dm^{-3} (Fig. 3). Values of the area per molecule at zero surface pressure, A_1, were determined by drawing a tangent from the linear segments of the final rising portions of the π–A isotherms to the zero abscissa (Table 1). Apparently, A_1 depends on the composition of the subphase solution and increases in the order: water < adenine < adenosine < ATP solution. Thus, one may postulate that the respective complexes of the adduct and the base are formed in films because the larger the size of the base molecule the more area demanding is the complex. Also, values of compressibility, $\kappa = -(1/A_1)(\mathrm{d}A/\mathrm{d}\pi)_T$, where T is the Kelvin temperature, were calculated at A_1 from reciprocal slopes of the linear segments of the π–A isotherms (Table 1). These κ values, being virtually independent of the subphase composition, indicate the formation of "expanded liquid" type films at the water–air interface.[17] For all subphase compositions, the A_1 value increases with the decrease of the sample volume of the spread adduct solution, as shown by way of example for the ATP subphase solution in Fig. 4. Moreover, this increase is more pronounced the larger the area of the C_{60}-uracil–base complex at horizontal orientation (Table 2). This type of concentration dependence of A_1 is typical for aggregated films. Therefore, the A_1 values were linearly extrapolated for all systems (Fig. 5), with correlation coefficient, $R \geqslant 0.98$, to the zero adduct amount in the films in order to determine values of the surface area per molecule at the infinite adduct dilution in

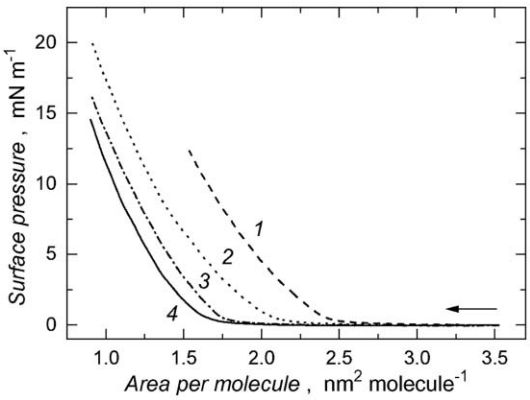

Fig. 3 Langmuir trough isotherms of surface pressure *vs.* area per molecule for a 0.2 mL sample of 0.114 mmol dm^{-3} C_{60}-uracil in chloroform spread onto subphase of (*1*) 1.81 mmol dm^{-3} ATP, (*2*) 1.81 mmol dm^{-3} adenosine, (*3*) 1.81 mmol dm^{-3} adenine, (*4*) water.

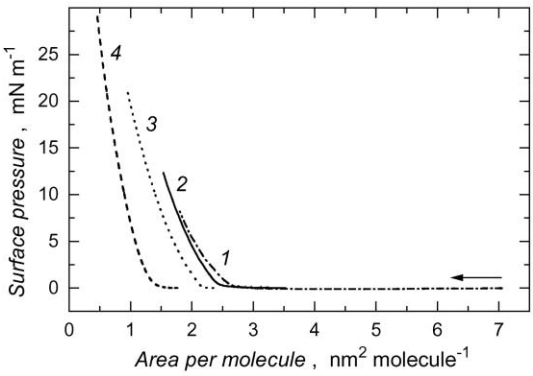

Fig. 4 Langmuir trough isotherms of surface pressure *vs.* area per molecule for (*1*) 0.1, (*2*) 0.2, (*3*) 0.3 and (*4*) 0.4 ml of 0.114 mmol dm^{-3} C_{60}-uracil in chloroform spread onto 1.81 mmol dm^{-3} ATP subphase solution.

Table 1 Area per molecule at zero surface pressure (A_1), compressibility (κ), and a dipole moment component normal to the air–water interface ($\mu_\perp$), for the Langmuir films of C_{60}-uracil spread from the 0.2 mL samples of 0.114 mmol dm^{-3} C_{60}-uracil in chloroform onto subphase solutions of different compositions

			$\mu_\perp$ (D)		
			Calculated[a]		
Subphase composition	A_1/nm^2 molecule^{-1}	κ/m mN^{-1}	Vertical orientation	Horizontal orientation	Determined (±0.2 D st. dev.)
Water	1.50	0.023	−3.7	3.2	1.8
1.81 mmol dm^{-3} Adenine	1.65	0.023	−3.5	1.2	1.3
1.81 mmol dm^{-3} Adenosine	1.79	0.022	−7.4	3.6	1.5
1.81 mmol dm^{-3} ATP	2.15	0.023	−3.9	1.6	1.4

[a]Semi-empirical calculations with PM3 parameterization for molecules in vacuum.

Table 2 Area per molecule for C_{60}-uracil and its complex containing adenine, adenosine or ATP, A_0, both calculated and determined by extrapolation of the Langmuir A_1 values to the zero adduct concentration in the film (*cf.* Fig. 5)

	A_0/nm^2		
	Calculated for complex C_{60}-uracil: base		
Subphase solution	Vertical orientation	Horizontal orientation	Extrapolated (*cf.* Fig. 5)
H_2O	1.19	1.45	1.9 ± 0.1
Adenine	1.19	1.54	2.3 ± 0.1
Adenosine	1.44	2.06	2.7 ± 0.1
ATP	1.57	2.95	3.0 ± 0.1

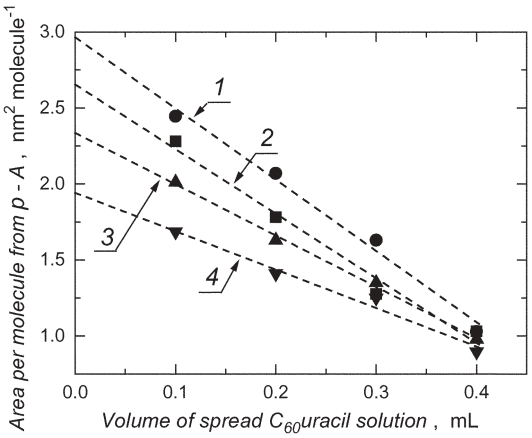

Fig. 5 Dependence of area per molecule at zero surface pressure on volume of the spread sample of 0.114 mmol dm^{-3} C_{60}-uracil in chloroform for subphase solution of (*1*) 1.81 mmol dm^{-3} ATP, (*2*) 1.81 mmol dm^{-3} adenosine, (*3*) 1.81 mmol dm^{-3} adenine, (*4*) water.

the films, A_0, (Table 2). In order to propose orientation of molecules in the films, the determined A_0 values were compared with those calculated both for the vertical and horizontal orientation of the adduct and complex by taking into account the van der Waals atomic radii (Table 2). Clearly, the extrapolated A_0 values are closer to the calculated A_0 values for horizontal rather than vertical orientation.

The conclusion on horizontal orientation was also supported by relatively low but positive values of the dipole moment component vertical to the interface for all subphase compositions and all amounts of **1** present in the films. This component was calculated by using the Helmholtz equation,[18] $\mu_\perp = \Delta V A \varepsilon_0$ (ε_0 is electric permittivity of vacuum and ΔV is the surface potential change due to the film formation estimated from heights of the rather small and ill-developed steps in the ΔV–A isotherms (not shown) (Table 1). Interestingly, the surface potential change starts to increase during the film compression at much lower values of area per molecule than those at which the corresponding surface pressure increases in the π–A isotherms and the upper inflection points in the ΔV–A isotherms correspond to the initial rising portions of the π–A isotherms. Positive $\mu_\perp$ values for all subphase solutions indicate that dipole moment vectors are directed from the solution to air phase. The $\mu_\perp$ values were also estimated by semi-empirical PM3 methods for the adduct and its complexes in the gas phase (Table 1). Importantly, the determined $\mu_\perp$ values are in accord with those calculated for horizontal (positive values) rather than vertical (negative values) orientation. This negative sign of $\mu_\perp$ would mean that the vector of the dipole moment is directed from the air toward solution phase corresponding to orientation of the hydrophilic part of the adduct (on water) or the complex (on the base solution) toward solution and hydrophobic part toward air. However, positive rather than negative changes of the surface potential were obtained during the film compression for all systems which indicates that vertical orientation is unlikely.

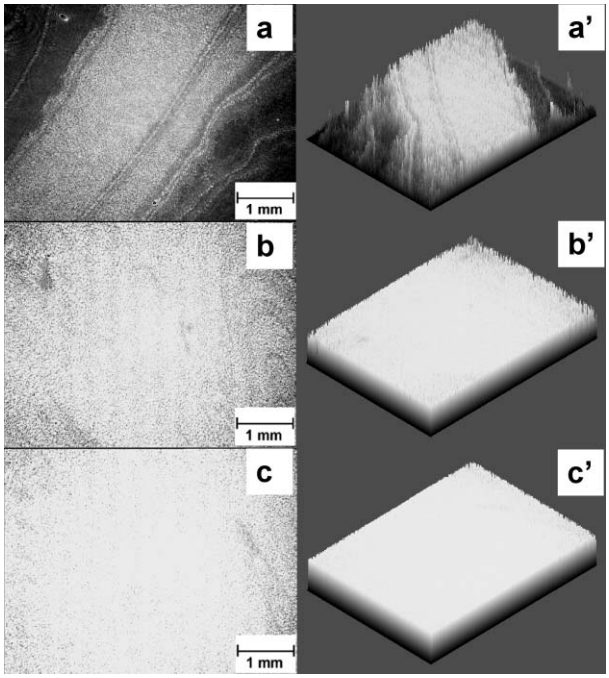

Fig. 6 (a), (b) and (c) top as well as (a′), (b′) and (c′) pseudo 3D views of Brewster angle microscopy images of C_{60}-uracil film floating on a 1.81 mmol dm^{-3} adenine subphase solution for surface pressure (a) and (a′) 0 mN m^{-1}, (b) and (b′) 5 mN m^{-1} as well as (c) and (c′) 15 mN m^{-1}; a spread sample was 0.3 mL of 0.114 mmol dm^{-3} C_{60}-uracil in chloroform.

Noticeably, relatively stable films of both the adduct and its complexes are obtained with no collapse points in the attainable surface pressure range, *i.e.*, $0 \leqslant \pi \leqslant 30$ mN m^{-1}, both for all compositions of the subphase solutions and amounts of **1** spread. Furthermore, no plateaus appear on the π–A isotherms under any solution or pressure conditions. Moreover, the compression of the **1** film floating on either of the subphase solution studied is reversible. That is, no hystereses in the π–A isotherms are observed in the compression–expansion cycles if the pressure reversal is set at $\pi \leqslant$ 20 mN m^{-1}.

A Brewster microscopy image of the film of **1** in the course of compression, shown by way of example for the adenine subphase solution in Fig. 6, reveals condensed phase domains which move closer one to the other and, eventually, make a uniform film at sufficiently high surface pressure. This behavior is different from the Langmuir films of genuine C_{60} for which foam-like features with circular domains were observed[9f] and also, from the films of some ester derivatives of C_{60} for which rod-type features were observed.[9d]

UV-visible absorption spectral characterization of Langmuir–Blodgett films of the C_{60}-uracil base paired complexes

The Langmuir films were transferred under a constant surface pressure of 15 mN m^{-1}, by using the LB technique in the emersion mode onto quartz slides for the UV-visible spectroscopy examination. The UV-visible spectra were recorded for the LB films after each indicated number of the immersion–emersion cycles in which certain number of monolayers were transferred. Absorption at 560 nm of the films of **1** increases with the number of the immersion–emersion cycles indicating that the Lambert–Beer law is obeyed for all films and, hence, the number of immersion–emersion cycles corresponds to the

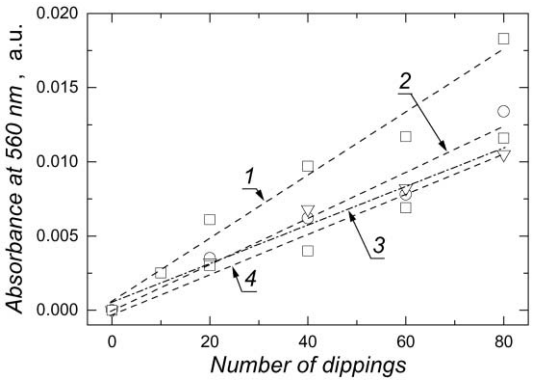

Fig. 7 Dependence of electronic absorption at 560 nm of the C_{60}-uracil LB films, transferred onto quartz slides by emersion, on the number of immersion–emersion cycles from subphase of (*1*) water, (*2*) 1.81 mmol dm^{-3} adenine, (*3*) 1.81 mmol dm^{-3} adenosine and (*4*) 1.81 mmol dm^{-3} ATP.

number of monolayers transferred (Fig. 7). Importantly, absorption of the adduct films transferred from water is markedly larger than those transferred from either of the base subphase solutions at the same number of monolayers transferred. At 560 nm absorption is solely due to the C_{60} part of the adduct. Hence, undoubtedly, more of the adduct in the film is transferred from water than from the base solution. This result qualitatively agrees with the smaller surface area per molecule occupied by the adduct floating on pure water than that of its complex floating on a base-containing subphase solution, determined for the Langmuir films of **1** (Table 1).

4 Conclusions

We have successfully demonstrated base pairing of adenine, adenosine, or adenosine 5′-triphosphate (ATP) by a newly synthesized C_{60}-uracil adduct *via* complementary hydrogen bonding at the air–water interface. Molecular modeling by *ab initio* B3LYP/3-21G(*) calculations, revealed Watson–Crick type complementary base pairing. The Langmuir trough studies of the C_{60}-uracil–adenine, C_{60}-uracil–adenosine and C_{60}-uracil–ATP complexes characterized by isotherms of surface pressure *versus* area per molecule, revealed formation of the ''expanded liquid'' type films. The calculated area per molecule at infinite adduct dilution in the film was dependent on the composition of the subphase solution and increased in the order: water < adenine < adenosine < ATP suggesting horizontal orientation of the complexes in the films. The Brewster angle microscopy imaging of the Langmuir films and the UV-visible spectral characterization of the LB films yielded additional information on morphology and stability, respectively, of the base-paired complexes.

Acknowledgement

The authors are thankful to the donors of the Petroleum Research Fund, administered by the American Chemical Society, the National Institutes of Health (GM 59038), National Science Foundation (CCLI and A&I) and NATO for support of this work. The High Performance Computing Center of the Wichita State University for lending SGI ORIGIN 2000 computer time is also acknowledged. Vu T. Hoang is thankful to the McNair Scholars Program for an undergraduate minority student scholarship.

References

1 B. Alerts, D. Bray, J. Lewis, M. Raff, K. Roberts and J. D. Watson, *Molecular Biology of the Cell*, 2nd ed. Garland Publishing, New York, 1989.

2 (*a*) A. D. Hamilton, *Advances in Supramolecular Chemistry*, JAI Press, Greenwich, CT, USA, 1990; (*b*) D. Philip and J. F. Stoddart, *Angew. Chem., Int. Ed. Engl.*, 1996, **35**, 1154; (*c*) S. C. Zimmerman, *Top. Curr. Chem.*, 1993, **165**, 71; (*d*) J. Rebek, Jr, *Acc. Chem. Res.*, 1990, **23**, 399; (*e*) J.-M. Lehn, in *Supramolecular Chemistry: Concepts and Perspectives*, VCH, Weinheim, 1995; (*f*) Papers in the special issue on molecular recognition of *Chem. Rev*. 1997, **97**, 1231.

3 (*a*) J. R. Lakowicz, *Principles of Fluorescence Spectroscopy*, 2nd ed. Kluwer Academic, New York, 1999, Chapter 21; (*b*) M. D. Ward, *Chem. Soc. Rev.*, 1997, **26**, 365 and references therein; (*c*) T. Hayashi and H. Ogoshi, *Chem. Soc. Rev.*, 1997, **26**, 355; (*d*) M.-J. Blanco, M. C. Jimenez, J.-C. Chambron, V. Heitz, M. Linke and J.-P. Sauvage, *Chem. Soc. Rev.*, 1999, **28**, 293.

4 For yearly progress reports see: *Fullerene, Proc. Electrochem. Soc.* 1994–2001, **1–11**. Electrochemical Society, Pennington, NJ, USA.

5 (*a*) T. Da. Ros and M. Prato, *Chem. Commun.*, 1999, 663; (*b*) S. R. Wilson, in *''The Fullerene Handbook''*, Eds. K. M. Kadish and R. Ruoff, pp. 437–465, Wiley, New York, USA, 2000; (*c*) A. W. Jensen, S. R. Wilson and D. I. Shuster, *Bioorg. Med. Chem.*, 1996, **4**, 767.

6 (*a*) F. Prat, C.-C. Hou and C. S. Foote, *J. Am. Chem. Soc.*, 1997, **119**, 5051; (*b*) R. Bernstein, F. Prat and C. S. Foote, *J. Am. Chem. Soc.*, 1999, **121**, 464.

7 (*a*) H. Tokuyama, S. Yamago, E. Nakamura, T. Shiraki and Y. Sugiura, *J. Am. Chem. Soc.*, 1993, **115**, 7918; (*b*) E. Nakamura, H. Tokuyama, S. Yamago, T. Shiraki and Y. Sugiura, *Bull. Chem. Soc. Jpn.*, 1996, **69**, 2143; (*c*) Y. N. Yamakoshi, T. Yagami, S. Sueyoshi and N. Miyata, *J. Org. Chem.*, 1996, **61**, 7236; (*d*) T. Mashino, K. Okuda, T. Hirota, M. Hirobe, T. Nagano and M. Mochizuchi, *Bioorg. Med. Chem. Lett.*, 1999, **9**, 2959; (*e*) Y. Tabata, Y. Murakami and Y. Ikada, *Fullerene Sci. Technol.*, 1997, **5**, 989; (*f*) Y. Tabata, Y. Murakami and Y. Ikada, *Jpn. J. Cancer. Res.*, 1997, **88**, 1108; (*g*) S. Samal, B.-J. Choi and K. E. Geckeler, *Chem. Commun.*, 2000, 1373; (*h*) A. S. Boutorine, H. Tokuyama, M. Takasugi, H. Isobe, E. Nakamura and C. Helene, *Angew. Chem., Int. Ed. Engl.*, 1994, **23–24**, 2462; (*i*) Y. Z. An, C. H. B. Chen, J. L. Anderson, D. S. Sigman, C. S. Foote and Y. Rubin, *Tetrahedron*, 1996, **52**, 5179; (*j*) M Bergamin, T. Da. Ros, G. Spalluto, A. Boutorine and M. Prato, *Chem. Commun.*, 2001, 17; (*k*) E. Nakamura, H. Isobe, N. Tomita, M. Sawamura, S. Jinno and H. Okayama, *Angew. Chem., Int. Ed. Engl.*, 2000, **39**, 4254.

8 K. Agira and T. Kunitake, *Acc. Chem. Res.*, 1998, **31**, 371.

9 (*a*) For a review, see: C. A. Mirkin and W. B. Caldwell, *Tetrahedron*, 1996, **52**, 5113; (*b*) M. Prato, *J. Mater. Chem.*, 1997, **7**, 1097; (*c*) R. A. J. Janssen, M. P. T. Christiaans, K. M. Pakbaz, D. Moses, T. C. Hummelen and N. S. Sariciftc, *J. Chem. Phys.*, 1995, **102**, 2628; (*d*) D. M. Guldi, Y. Tian, J. H. Fendler, H. Hungerbühler and K. D. Asmus, *J. Phys. Chem*, 1996, **100**, 2753; (*e*) P. Wang, Y. Maruyama and R. M. Metzger, *Langmuir*, 1996, **12**, 3932; (*f*) R. Castillo, S. Ramos and J. Ruiz-Garcia, *J. Phys. Chem.*, 1996, **100**, 15235; (*g*) D. Zhou, L. Gan, C. Luo, H. Tan, C. Huang, G. Yao, X. Zhao, Z. Liu, X. Xia and B. Zhang, *J. Phys. Chem.*, 1996, **100**, 3150; (*h*) M. I. Sluch, I. D. W. Samuel and M. C. Petty, *Chem. Phys. Lett.*, 1997, **280**, 315; (*i*) T. Kawai, S. Scheib, M. P. Cava and R. M. Metzger, *Langmuir*, 1997, **13**, 5627; (*j*) S. Wang, R. M. Leblanc, F. Arias and L. Echegoyen, *Langmuir*, 1997, **13**, 1672; (*k*) D. Zhou, G. J. Ashwell, R. Rajan, L. Gan, C. Luo and H. Chunhir, *J. Chem. Soc., Faraday Trans.*, 1997, **93**, 2077; (*l*) M. I. Sluch, I. D. W. Samuel, A. Beeby and M. C. Petty, *Langmuir*, 1998, **14**, 3343; (*m*) N. Takashi, M. Hiroto and N. Naotoshi, *Chem. Lett.*, 1998, **12**, 1219; (*n*) F. Cardullo, F. Diederich, L. Echegoyen, T. Habicher, N. Jayaraman, R. M. Leblanc, J. F. Stoddart and S. Wang, *Langmuir*, 1998, **14**, 1955; (*o*) W. Zhang, Y. Shi, L. Gan, C. Huang, H. Luo, D. Wu and N. Li, *J. Phys. Chem. B*, 1999, **103**, 675; (*p*) M. Maggini, A. Karlsoon, L. Pasimeni, G. Scorrano, M. Prato and L. Valli, *Tetrahedron Lett.*, 1994, **35**, 2985; (*q*) M. Maggini, M. Pasimeni, M. Prato, G. Scorrano and L. Valli, *Langmuir*, 1994, **10**, 4164; (*r*) D. Zhou, L. Gan, C. Luo, C. Huang and Y. Wu, *Solid State Commun.*, 1997, **102**, 891; (*s*) D. M. Guldi, M. Maggini, S. Mondini, F. Guerin and J. H. Fendler, *Langmuir*, 2000, **16**, 1311; (*t*) W. Kutner, K. Noworyta, G. R. Deviprasad and F. D'Souza, *Mol. Cryst. Liq. Cryst. Sci. Technol., Sect. C*, 2000, **13**(1–4), 295; (*u*) K. Noworyta, W. Kutner, G. R. Deviprasad and F. D'Souza, *Synth. Met.*, 2002, in press.

10 M. Maggini, G. Scorrano and M. Prato, *J. Am. Chem. Soc.*, 1993, **115**, 9798.

11 *Gaussian 98* (Revision A.7), M. J. Frisch, G. W. Trucks, H. B. Schlegel, G. E. Scuseria, M. A. Robb, J. R. Cheeseman,

V. G. Zakrzewski, J. A. Montgomery, R. E. Stratmann, J. C. Burant, S. Dapprich, J. M. Millam, A. D. Daniels, K. N. Kudin, M. C. Strain, O. Farkas, J. Tomasi, V. Barone, M. Cossi, R. Cammi, B. Mennucci, C. Pomelli, C. Adamo, S. Clifford, J. Ochterski, G. A. Petersson, P.Y. Ayala, Q. Cui, K. Morokuma, D. K. Malick, A. D. Rabuck, K. Raghavachari, J. B. Foresman, J. Cioslowski, J. V. Ortiz, B. B. Stefanov, G. Liu, A. Liashenko, P. Piskorz, I. Komaromi, R. Gomperts, R. L. Martin, D. J. Fox, T. Keith, M. A. Al-Laham, C. Y. Peng, A. Nanayakkara, C. Gonzalez, M. Challacombe, P. M. W. Gill, B. G. Johnson, W. Chen, M. W. Wong, J. L. Andres, M. Head-Gordon, E. S. Replogle, J. A. Pople, Gaussian, Inc., Pittsburgh, PA, USA,1998

12 W. Kutner, K. Noworyta, G. R. Deviprasad and F. D'Souza, *J. Electrochem. Soc.*, 2000, **147**, 2647 and references therein.

13 (*a*) F. D'Souza, M. E. Zandler, P. M. Smith, G. R. Deviprasad, K. Arkady, M. Fujitsuka and O Ito, *J. Phys. Chem. A*, 2002, **106**, 649; (*b*) F. D'Souza, G. R. Deviprasad, M. E. Zandler, V. T. Hoang, K. Arkady, M. VanStipdonk, A. Perera, M. E. El-Khouly, M. Fujitsuka and O. Ito, *J. Phys. Chem. A.*, 2002, **106**, 3243.

14 F. D'Souza, N. P. Rath, G. R. Deviprasad and M. E. Zandler, *Chem. Commun.*, 2001, 267.

15 J. Sponer and P. Hobza, *J. Phys. Chem. A*, 2000, **104**, 4592.

16 S. Kawahara, T. Uchimaru, K. Taira and M. Sekine, *J. Phys. Chem. A*, 2001, **105**, 3894.

17 (*a*) J. Pranata, S. G. Wierschke and W. L. Jorgensen, *J. Am. Chem. Soc.*, 1991, **113**, 2810; (*b*) T. J. Murry and S. C. Zimmerman, *J. Am. Chem. Soc.*, 1992, **114**, 4010.

18 (*a*) T. Smith, *J. Colloid Interface Sci.*, 1992, **23**, 27; (*b*) V. Vogel and D. Möbius, *J. Colloid Interface Sci.*, 1988, **126**, 408.